General formula for coupling-loss characterization of single-mode fiber collimators by use of gradient-index rod lenses

Shifu Yuan and Nabeel A. Riza

A general formula for determining the coupling loss between two single-mode fiber collimators with the simultaneous existence of separation, lateral offset and angular tilt misalignments, and spot-size mismatch is theoretically derived by use of the Gaussian field approximation. Based on this general formula, the formulas for coupling losses that are due to the misalignment of insert separation, lateral offset, and angular tilt are given. The formula for the coupling loss that is due to Gaussian spot-size mismatch of two single-mode collimators is also given. Good agreement between these formulas and experimental results is demonstrated with gradient-index rod lens-based fiber collimators operating in the 1300-nm band. © 1999 Optical Society of America

OCIS codes: 060.2310, 060.2340, 060.2430, 110.2760.

1. Introduction

Free-space-based fiber-optic components such as isolators, circulators, attenuators, switches, and wavelength-division multiplexers/demultiplexers have become key devices for optical fiber communications, optical fiber sensing, and radio-frequency photonics.[1–4] In these free-space-based fiber-optic components, single-mode-fiber (SMF) or multimode-fiber pigtailed fiber collimators have been widely used. This is so because the coupling between two fiber collimators has a large allowable separation distance with a low loss[5,6] that is critical for a practical free-space interconnected fiber-optic module or subsystem. However, to maintain low coupling loss requires that the separation distance between two fiber collimators be limited. An important engineering issue that is related to the use of fiber collimators is the excess loss performance of a pair of collimators owing to misalignment between the collimating and the focusing gradient-index (GRIN) lenses. There are three types of misalignment that introduce insertion loss into the coupling, i.e., separation misalignment between the lens surfaces, offset misalignment between the longitudinal axes of the lenses, and angular tilt misalignment between the longitudinal axes of the lenses. Gaussian beam spot-size mismatch also causes insertion loss.

One can determine the coupling loss of two multimode fiber collimators by calculating the overlap area of the output beams of the two collimators.[5] For SMF collimators, one must use the Gaussian field approximation method[7–9] to characterize the coupling loss rather than calculate the overlap area, and three formulas to describe the coupling loss that is due to only one of the three misalignments have been reported.[6] Based on these formulas, a fiber array optical coupling design issue for a photonic beam formation system has been reported.[10] However, those formulas are not suitable for describing the coupling-loss performance of fiber collimators with large separation (>10 cm) and large lateral offset (>300 μm). In addition, they cannot characterize the coupling-loss performance when the three misalignments and spot-size mismatch exist simultaneously. Hence in this paper we analyze the coupling-loss characteristics of fiber collimators with simultaneous three misalignments and spot-size mismatch and give a general formula to describe the coupling-loss performance. Experimental results show that this for-

When this research was performed, both authors were with the Center for Research and Education in Optics and Lasers and the School of Optics, University of Central Florida, P.O. Box 162700, 4000 Central Florida Boulevard, Orlando, Florida 32816-2700. S. Yuan is now with Chorum Technologies, Incorporated, 1155 East Collins Boulevard, Suite 200, Richardson, Texas 75081. The e-mail address for N. A. Riza is riza@creol.ucf.edu; for S. Yuan it is shyuan@chorumtech.com.
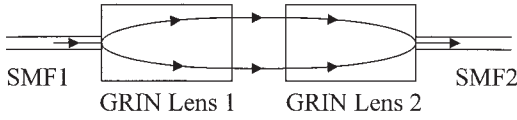
Fig. 1. Fiber coupling system using two quarter-pitch SMF collimators.

mula is adequate for predicting the coupling losses that are due to the three kinds of misalignment.

2. Gaussian Field Approximation of Light Propagation in Quarter-Pitch Gradient-Index Lenses

Figure 1 shows the fiber coupling system with two SMF collimators. GRIN lens 1 is a transmitting lens, and GRIN lens 2 is a receiving lens or focusing lens. It is well known that the light-field distribution of the fundamental mode in a SMF can be well approximated by a Gaussian profile.[7–9] The Gaussian beam from SMF1 is collimated by GRIN lens 1 and then focused into the output SMF2. Gaussian beam propagation in the fiber collimating system is shown schematically in Fig. 2. For a fiber collimator using a quarter-pitch GRIN lens the fiber is butt attached to the GRIN lens. The optical field emitted from SMF1 can be approximated by a Gaussian beam whose waist coincides with the end surface of SMF1. The fundamental-mode Gaussian beam can be described with its Gaussian spot size (Gaussian beam radius) w_i and radius of curvature R_i of equiphase surfaces. Combining the two parameters, we have a complex curvature parameter q_i:

$$\frac{1}{q_i} = \frac{1}{R_i} - j\frac{\lambda}{\pi n w_i^2}, \tag{1}$$

where λ is the wavelength of light in vacuum and n is the refractive index of the medium in the gap.[11]

The GRIN rod lens has its largest refractive index along the longitudinal axis, and the refractive index decreases quadratically with radial distance. The refractive index can be expressed as

$$n(r) = n_0\left(1 - \frac{Ar^2}{2}\right), \tag{2}$$

where n_0 is the refractive index on the axis of the lens, $\sqrt{A}$ is the gradient constant, and r is the radial distance from the central axis.
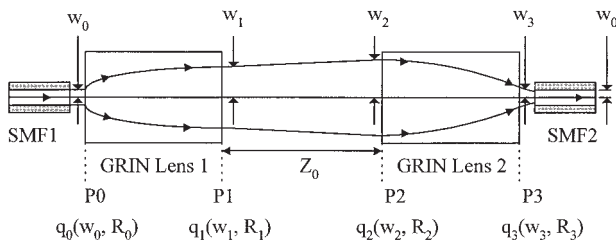

Fig. 2. Gaussian beam propagation in the fiber collimating system.

The GRIN lens has the ray matrix

$$\begin{bmatrix} \cos(\sqrt{A}Z) & \frac{1}{n_0\sqrt{A}}\sin(\sqrt{A}Z) \\ -n_0\sqrt{A}\sin(\sqrt{A}Z) & \cos(\sqrt{A}Z) \end{bmatrix}, \tag{3}$$

where Z is the length of the GRIN lens.[12] The pitch of a GRIN lens is defined as $p = \sqrt{A}\,Z/(2\pi)$. For a quarter-pitch GRIN lens, i.e., $p = 1/4$, we have $\sqrt{A}\,Z = \pi/2$. Thus the ray matrix of a quarter-pitch GRIN lens can be expressed as

$$G = \begin{bmatrix} A_1 & B_1 \\ C_1 & D_1 \end{bmatrix} = \begin{bmatrix} 0 & \frac{1}{n_0\sqrt{A}} \\ -n_0\sqrt{A} & 0 \end{bmatrix}. \tag{4}$$

Note that both GRIN lens 1 and GRIN lens 2 have the same ray matrix.

The gap with a straight length of Z_0 between GRIN lens 1 and GRIN lens 2 has a ray matrix[11] of

$$S = \begin{bmatrix} A_2 & B_2 \\ C_2 & D_2 \end{bmatrix} = \begin{bmatrix} 1 & Z_0 \\ 0 & 1 \end{bmatrix}. \tag{5}$$

It is well known that a Gaussian beam propagates in terms of the $ABCD$ law[11]

$$q_{i+1} = \frac{A_i q_i + B_i}{C_i q_i + D_i}. \tag{6}$$

Considering that the Gaussian optical field emitted from SMF1 has a modal field diameter of w_0 with $R_0 = \infty$, and using the $ABCD$ law [i.e., Eq. (6)] and Eqs. (1), (4), and (5), we have

$$w_1 = \frac{\lambda}{\pi n w_0 n_0 \sqrt{A}}, \tag{7}$$

$$R_1 = \infty, \tag{8}$$

$$w_2 = w_1\left[1 + \left(\frac{\lambda Z_0}{\pi n w_1^2}\right)^2\right]^{1/2}, \tag{9}$$

$$R_2 = Z_0\left[1 + \left(\frac{\pi n w_1^2}{\lambda Z_0}\right)^2\right], \tag{10}$$

$$w_3 = \frac{\lambda}{n_0\sqrt{A}\pi n w_1} = w_0, \tag{11}$$

$$R_3 = -\frac{1}{n_0(\sqrt{A})^2 Z_0}. \tag{12}$$

According to the derivations in Eqs. (7)–(12), we have arrived at unique results for the coupling property of SMF collimators compared with those described in Ref. 6. The light beam emitted from GRIN lens 1 is a Gaussian beam with its Gaussian waist at the surface of the lens. When the Gaussian beam propagates to the surface of GRIN lens 2, the beam spot size is w_2 expanded with radius of curvature R_2. For the beam at output surface P3 of GRIN lens 2, the spot size is $w_3 = w_0$; i.e., it has the same
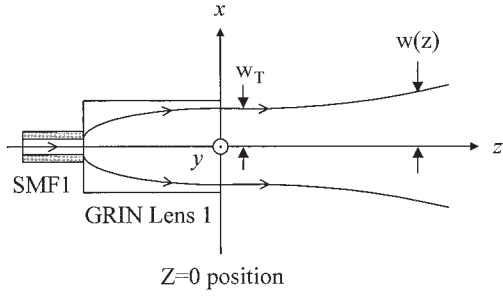
Fig. 3. Output optical field distribution from GRIN lens 1.

Fig. 4. Equivalent optical field distribution that can be perfectly coupled into the SMF2 by use of GRIN lens 2.

spot size as the modal field radius of the fundamental mode in the SMF. The coupling loss results from the different radii of curvature; i.e., the perfectly aligned light beam coupled into the fiber should have a spot size w_0 with a radius $R = \infty$, whereas the beam from GRIN lens 2 has a spot size w_0 with a radius $R = -1/[n_0(\sqrt{A})^2 Z_0]$. When Z_0 increases, $|R|$ decreases, so collecting the beam to have good coupling requires a fiber with a bigger numerical aperture. Thus when we are considering such a fiber–fiber lens-coupling issue, we must take into account the radius of curvature of the Gaussian beam because considering only the spot size cannot give us a good approximation to determine coupling loss.

3. Coupling-Loss Formula

Consider the output field from GRIN lens 1 shown in Fig. 3. The Gaussian beam waist is denoted w_T. The surface of GRIN lens 1 is the waist position. The x component E_x of the Gaussian light-field vector can be expressed as[11]

$$
E_x(x, y, z) = E_1 \frac{w_T}{w(z)} \exp\left\{-i[kz - \eta(z)] \right.
$$
$$
\left. - r^2 \left[\frac{1}{w^2(z)} + i\frac{k}{2R(z)}\right]\right\}, \quad (13)
$$

where E_1 is the output field's amplitude at the origin position $(x = 0, y = 0, z = 0)$, r is the radius from position (x, y, z) to the z axis,

$$
k = 2\pi n/\lambda, \quad (14)
$$

$$
\eta(z) = \tan^{-1}\left(\frac{\lambda z}{\pi n w_T^2}\right), \quad (15)
$$

$$
w^2(z) = w_T^2\left[1 + \left(\frac{\lambda z}{\pi n w_T^2}\right)^2\right], \quad (16)
$$

$$
R(z) = z\left[1 + \left(\frac{\pi n w_T^2}{\lambda z}\right)^2\right]. \quad (17)
$$

Note that the time factor $\exp(i\omega t)$ is omitted from Eq. (13). For coupling-loss analysis we must consider two fiber collimators because the loss is due to misalignment and mismatch of the two GRIN collimators. Although the light beam emitted from GRIN lens 1 goes through the gap and GRIN lens 2 and reaches SMF2, only an effective beam equivalent
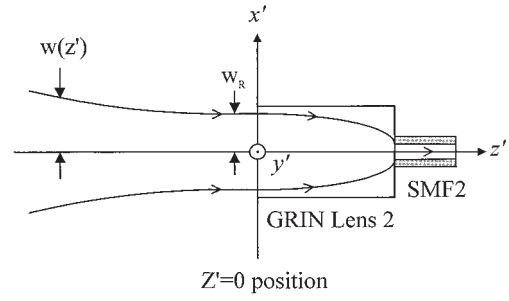
to the fundamental mode in SMF2 can be coupled into the fiber, as shown in Fig. 4. Omitting the time factor $\exp(i\omega t)$, we can express the x' component $E_{x'}$ of the light field of the effective equivalent beam in the gap as

$$
E_{x'}(x', y', z') = E_1 \frac{w_T}{w(z')} \exp\left\{-i[kz' - \eta(z')]\right.
$$
$$
\left. - r'^2\left[\frac{1}{w^2(z')} + i\frac{k}{2R(z')}\right]\right\}, \quad (18)
$$

where r' is the radius from position (x', y', z') to the z' axis,

$$
\eta(z') = \tan^{-1}\left(\frac{\lambda z'}{\pi n w_R^2}\right), \quad (19)
$$

$$
w^2(z') = w_R^2\left[1 + \left(\frac{\lambda z'}{\pi n w_R^2}\right)^2\right], \quad (20)
$$

$$
R(z') = z'\left[1 + \left(\frac{\pi n w_R^2}{\lambda z'}\right)^2\right]. \quad (21)
$$

Note that in Eq. (18) we have considered energy conservation for the coupling, so the expression has an E_1 and a w_T factor. The coupling loss between the two collimators can be determined by the coupling coefficient between the two Gaussian beams. Coupling loss is determined by separation, offset, and angular misalignments of the two Gaussian beams, as shown in Figs. 5(a), 5(b), and 5(c), respectively. It should be pointed out the coupling loss that is due to these misalignments includes the loss that is due to the Gaussian beam spot-size mismatch because the two SMF collimators have different Gaussian beam radii. Figure 6 shows a side view of two fiber collimators with the three combined misalignments and spot-size mismatch in two rectangular systems (x, y, z) and (x', y', z'). The coupling coefficient η_c at $z' = 0$ between the two Gaussian beams can be expressed as[7,9]

$$
\eta_c = \frac{2}{\pi E_1^2 w_T^2} \int_{-\infty}^{+\infty}\int_{-\infty}^{+\infty} E_x(x, y, z)|_{z'=0}
$$
$$
\times E_{x'}^*(x', y', z')|_{z'=0} \mathrm{d}x' \mathrm{d}y'. \quad (22)
$$

Note that there is a factor $2/(\pi E_1^2 w_T^2)$ in Eq. (22) whose function is to maintain $\eta_c = 1$ (i.e., for energy

conservation) when no misalignments exist. Although in Eq. (12) we consider only the E_x component, the same equation is suitable for the E_y component, so this coupling coefficient applies for all polarization directions. It is readily shown from Fig. 6 that the two rectangular coordinate systems are related by

$$x = x' \cos\theta - z' \sin\theta + X_0, \qquad (23)$$

$$z = x' \sin\theta + z' \cos\theta + Z_0, \qquad (24)$$

$$y = y', \qquad (25)$$

$$r^2 = x^2 + y^2 = (x' \cos\theta - z' \sin\theta + X_0)^2 + y'^2. \quad (26)$$

Considering $\cos\theta \approx 1$ when θ is very small (e.g., $\theta \leq 0.3°$, a typical case for GRIN lens misalignment with SMF coupling), we can replace z in $w(z)$ and $R(z)$ and $\eta(z)$ by Z_0 and put them into Eq. (13). For $z' = 0$, Eq. (13) can be rewritten as

$$E_x(x, y, z)|_{z'=0} = E_x(x' + X_0, y', x'\sin\theta + Z_0)$$

$$= E_1 \frac{w_T}{w(Z_0)} \exp\{-i[kZ_0 - \eta(Z_0)]\}$$

$$\times \exp\left(-\left\{\left[\frac{1}{w^2(Z_0)} + i\frac{k}{2R(Z_0)}\right]x'^2 + \left\{\left[\frac{1}{w^2(Z_0)} + i\frac{k}{2R(Z_0)}\right]\right.\right.$$

$$\times 2X_0 + ik\sin\theta\right\}x' + \left[\frac{1}{w^2(Z_0)} + i\frac{k}{2R(Z_0)}\right]X_0^2\right\}\right)$$

$$\times \exp\left\{-\left[\frac{1}{w^2(Z_0)} + i\frac{k}{2R(Z_0)}\right]y'^2\right\}. \quad (27)$$

Replacing r'^2 with $x'^2 + y'^2$ in Eq. (18) and considering the equivalent field distribution $E_{x'}$ at position $z' = 0$, we have

$$E_{x'}(x', y', z')|_{z'=0} = E_1 \frac{w_T}{w_R} \exp\left(-\frac{x'^2}{w_R^2}\right)\exp\left(-\frac{y'^2}{w_R^2}\right). \quad (28)$$
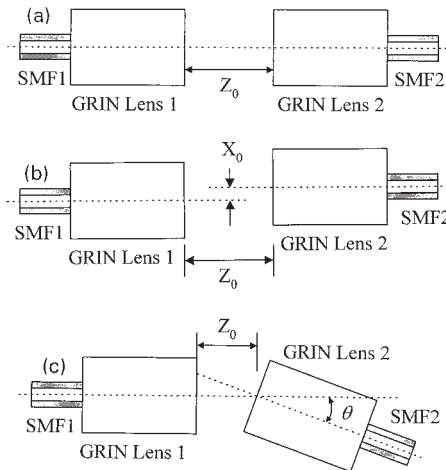
Fig. 5. (a) Separation misalignment between the two GRIN lens surfaces. (b) Offset misalignments between the longitudinal axes of the GRIN lenses. (c) Angular misalignments between the longitudinal axes of the GRIN lenses.
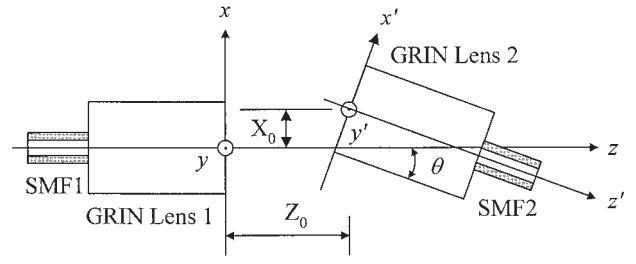
Fig. 6. Side view of two fiber collimators with three combined misalignments in two rectangular systems $[(x, y, z)$ and $(x', y', z')]$.

Putting Eqs. (27) and (28) into Eq. (22), and using the following integral[6]:

$$\int_{-\infty}^{+\infty} \exp[-(ax^2 + bx + c)]\mathrm{d}x = \sqrt{\frac{\pi}{a}} \exp\left[\frac{(b^2 - 4ac)}{4a}\right], \quad (29)$$

we can find the integral in Eq. (22) to be[9]

$$\eta_c = C_0 \exp\left[-\frac{A(C + jH)}{2B}\right]\exp(-j\psi_0), \quad (30)$$

where

$$C_0 = \left[\frac{4D}{B}\right]^{1/2}, \quad (31a)$$

$$\psi_0 = AG - \tan^{-1}\frac{G}{D + 1}, \quad (31b)$$

$$A = (kw_T)^2/2, \quad (31c)$$

$$B = G^2 + (D + 1)^2, \quad (31d)$$

$$C = (D + 1)F^2 + 2DFG \sin\theta$$
$$+ D(G^2 + D + 1)\sin^2\theta, \quad (31e)$$

$$D = (w_R/w_T)^2, \quad (31f)$$

$$F = \frac{2X_0}{kw_T^2}, \quad (31g)$$

$$G = \frac{2Z_0}{kw_T^2}, \quad (31h)$$

$$H = GF^2 - 2D(D + 1)F \sin\theta - GD^2 \sin\theta. \quad (31i)$$

The power transmission coefficient can be written as $T = |\eta_c|^2 = \eta_c\eta_c{}^*$. Putting Eqs. (31) into Eq. (30), we can calculate the power transmission coefficient T to be

$$T = \frac{4D}{B} \exp\left(-\frac{AC}{B}\right). \quad (32)$$

Thus the total coupling loss in decibels between two misaligned (i.e., three simultaneous misalignments) SMF collimators can be expressed as

$$L_{\mathrm{tot}}(X_0, Z_0, \theta) = -10 \log T$$

$$= -10 \log\left[\frac{4D}{B} \exp\left(-\frac{AC}{B}\right)\right]. \quad (33)$$

From these results we conclude that the loss performance between two fiber collimators is similar to the loss performance of two SMF's without fiber collimators.[9]

Specifically, by replacing the modal field radius of the SMF with the Gaussian beam radius in the formula for SMF coupling loss derived in Ref. 9, we can easily obtain the coupling-loss formula shown in Eq. (33). Note that, when no misalignments exist [i.e., $X_0 = 0$, $Z_0 = 0$, $\theta = 0$, and $w_R = w_T$ (no spot size mismatch)], from Eq. (33) we have $L_{\text{tot}}(X_0 = 0, Z_0 = 0, \theta = 0) = 0$ dB, which indicates the coupling loss owing to misalignments is 0 dB. This does not mean that in a perfect-alignment situation the coupling loss is 0 dB. In fact, some other factors such as the imperfection of GRIN lenses and backreflection of the lens surfaces cause additional coupling loss (e.g., 0.2–0.3 dB). This additional loss is not included in Eq. (33). To arrive at the total coupling loss of fiber collimators we must add this additional loss to Eq. (33).

Based on our general formula in Eq. (33), we can derive the normalized loss performances for the three kinds of fiber collimator misalignment with different Gaussian spot-size mismatch. The separation misalignment condition is shown in Fig. 5(a). The normalized coupling loss that is due to separation misalignment is

$$L_s = L_{\text{tot}}(X_0 = 0, Z_0, \theta = 0) - L_{\text{tot}}(X_0 = 0, Z_0 = 0, \theta = 0)$$

$$= -10 \log\left[\frac{4w_T^2 w_R^2}{\dfrac{\lambda^2 Z_0^2}{\pi^2 n^2} + (w_T^2 + w_R^2)^2}\right]. \tag{34}$$

The lateral offset misalignment condition is shown in Fig. 5(b). The normalized loss that is due to lateral offset misalignment at a specific separation distance Z_0 can be written as

$$L_l = L_{\text{tot}}(X_0, Z_0, \theta = 0) - L_{\text{tot}}(X_0 = 0, Z_0, \theta = 0)$$

$$= \frac{20}{\ln 10} \frac{n^2 \pi^2 (w_T^2 + w_R^2)}{\lambda^2 Z_0^2 + \pi^2 n^2 (w_T^2 + w_R^2)^2} X_0^2. \tag{35}$$

The angular tilt misalignment condition is shown in Fig. 5(c). The normalized loss that is due to angular offset misalignment at a specific separation distance Z_0 can be written as

$$L_a = L_{\text{tot}}(X_0 = 0, Z_0, \theta) - L_{\text{tot}}(X_0 = 0, Z_0, \theta = 0)$$

$$= \frac{20}{\ln 10} \frac{\left(\dfrac{n\pi w_R}{\lambda}\right)^2 \left[\left(\dfrac{\lambda Z_0}{\pi n w_T^2}\right)^2 + \left(\dfrac{w_R}{w_T}\right)^2 + 1\right]}{\left(\dfrac{\lambda Z_0}{\pi n w_T^2}\right)^2 + \left[\left(\dfrac{w_R}{w_T}\right)^2 + 1\right]^2} \sin^2 \theta. \tag{36}$$

Equation (33) also describes the loss performance that is due to Gaussian spot-size mismatch. If no other misalignment exists, the normalized loss that is
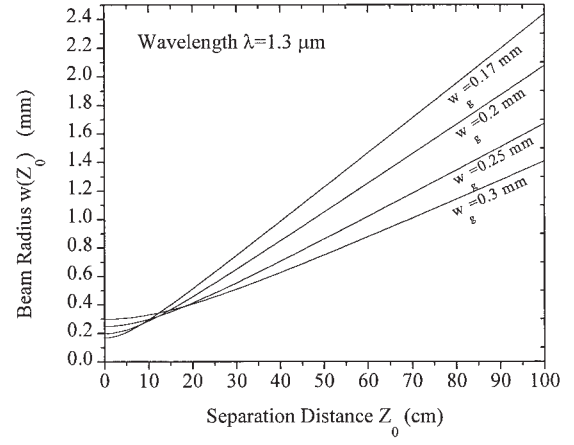

Fig. 7. Changing curves of beam radius $w(z)$ for several Gaussian waists w_g.

due only to spot-size mismatch (different w_T and w_R) can be derived as

$$L_m = L_{\text{tot}}(X_0 = 0, Z_0 = 0, \theta = 0, w_T, w_R)$$

$$- L_{\text{tot}}(X_0 = 0, Z_0 = 0, \theta = 0, w_T, w_R = w_T)$$

$$= -10 \log \frac{4}{\left(\dfrac{w_R}{w_T} + \dfrac{w_T}{w_R}\right)^2}. \tag{37}$$

4. Numerical Analysis

For GRIN lens free-space interconnections it is important to know the tolerance distance between two GRIN rod lenses. The tolerance distance is the maximum distance at which good coupling efficiency (e.g., <0.5 dB) can be achieved. This is especially true for free-space-based fiber-optic components such as fiber-optic circulators, isolators, matrix switches, and photonic delay lines. According to Eq. (34), the tolerance distance will be related to wavelength λ and the Gaussian beam widths at the output surface of the GRIN lens and to the refractive index n in the gap. When the beam width increases, the divergence of the beam decreases, so the tolerance distance becomes larger. With Eq. (16), Fig. 7 shows curves for beam radius $w(z)$ with several Gaussian waists w_g at $\lambda = 1.3$ µm. From the figure we can clearly see that when waist w_g becomes smaller, the divergence of the beam becomes larger. The divergence angle (half-apex angle) of a Gaussian beam can be given as $\theta_d = \tan^{-1}[\lambda/(\pi w_g n)] \approx \lambda/(\pi w_g n)$.[11] This relationship of divergence angle θ_d and Gaussian beam waist w_g is also shown in Fig. 8. Suppose that the fiber collimators are identical and that they have the same Gaussian waists $w_T = w_R = w_g$. Thus, using Eq. (34), we can write the insertion loss that is due to the separation distance as

$$L_s(Z_0) = 10 \log\left(1 + \frac{\lambda^2 Z_0^2}{4\pi^2 n^2 w_g^4}\right). \tag{38}$$

DOCKET ALARM

Explore Litigation Insights

Docket Alarm provides insights to develop a more informed litigation strategy and the peace of mind of knowing you're on top of things.

Real-Time Litigation Alerts

Keep your litigation team up-to-date with **real-time alerts** and advanced team management tools built for the enterprise, all while greatly reducing PACER spend.

Our comprehensive service means we can handle Federal, State, and Administrative courts across the country.

Advanced Docket Research

With over 230 million records, Docket Alarm's cloud-native docket research platform finds what other services can't. Coverage includes Federal, State, plus PTAB, TTAB, ITC and NLRB decisions, all in one place.

Identify arguments that have been successful in the past with full text, pinpoint searching. Link to case law cited within any court document via Fastcase.

Analytics At Your Fingertips

Learn what happened the last time a particular judge, opposing counsel or company faced cases similar to yours.

Advanced out-of-the-box PTAB and TTAB analytics are always at your fingertips.

API

Docket Alarm offers a powerful API (application programming interface) to developers that want to integrate case filings into their apps.

LAW FIRMS
Build custom dashboards for your attorneys and clients with live data direct from the court.

Automate many repetitive legal tasks like conflict checks, document management, and marketing.

FINANCIAL INSTITUTIONS
Litigation and bankruptcy checks for companies and debtors.

E-DISCOVERY AND LEGAL VENDORS
Sync your system to PACER to automate legal marketing.

fastcase
Smarter legal research.